Modeling Indoor TOA Ranging Error for Body Mounted Sensors

Jie He[◇†], Yishuang Geng[†] and Kaveh Pahlavan[†]

[◇]School of Computer & Communication Engineering
University of Science & Technology Beijing (USTB)
Beijing, China
hejie1983@gmail.com

[†]CWINS Laboratory, ECE department
Worcester Polytechnic Institute (WPI)
Wrocester, USA
{ygeng, Kaveh}@wpi.edu

***Abstract*—In Time of arrival (TOA) based indoor human tracking system, the human body mounted with the target sensor can cause non-line of sight (NLOS) scenario and result in significant ranging error. However, the previous studies on the behavior of indoor TOA ranging did not take the effects of human body into account. In this paper, we introduce a statistical TOA ranging error model for body mounted sensors based on the measurements in a typical office building. This model separates the ranging error into multipath error cased multipath combination and undetectable direct path (UDP) error derives from the body-caused NLOS. Both multipath error and UDP error are modeled as a Gaussian variable. The distribution of multipath error is relative to the bandwidth of the system and the distribution of UDP error is relative to the angle between the face direction and the direction of TX-RX, SNR and bandwidth of the system, clearly shows the effects of human body on TOA ranging.**

Keywords- TOA; Body area network; ranging error; human tracking; indoor localization; indoor location system.

I. INTRODUCTION

Position is one of the most important properties of human. It is critical to heath care and safety in many applications, such as the senior citizen's positions in a nursing home, patients' positions in the hospital, miners' positions in the underground mine, soldiers' positions in war and firefighters' positions in burning house [1]. The human tracking system is desired in these scenarios. In outdoor area, GPS can be used to provide the accurate position. In indoor areas or underground constructions, wireless indoor localization system is the most popular solution [1], in which the target sensor is mounted to human body and the distances between body surface and the base stations are measured to calculate target's position.

TOA is the most popular wireless indoor localization technology, much more accurate than Receive Signal Strength (RSS) based technology [9] and more practical than Angle of Arrival (AOA) based technology [2]. TOA estimates the distance by measuring the propagation time of the impulse between transmitter and receiver [4]. The accuracy of TOA ranging is correlated to the multipath condition of the wireless channel, since only the propagation time of the impulse in direct path represents the true distance. In a multipath rich environment, impulse always combines with the neighbor multipath components [3]. The direct path is unable to be distinguished and the most efficient way to estimate the arrival time of received signal is to measure the arrival time of the first peak above threshold in receive signal profile. In LOS scenario, the direct path is the strongest path and the ranging error comes from combination of the first detectable path and its neighbor paths, which is defined as multipath error. In NLOS scenario, except the multipath error, the lager error is caused by the blockage of direct path [4][6], which is defined as UDP error.

For localization of body mounted sensors, TOA ranging performs in the channel from body surface to base station, which is defined as CM4 for body area network in IEEE 802.15.6 standard [8][12-15]. In this particularly channel, the human body can cause NLOS [12] and results in significant UDP error. Therefore, human body is an important source of ranging error for body mounted sensors. However, the previous studies on the behavior of TOA ranging error in indoor environment [5][7][10][11] did not take the effects of human body into account.

In this paper, we present a statistical model of TOA ranging error for body mounted sensors based on measurements in a typical office environment. We model the distribution of TOA ranging error obtained from the measurement and relate the parameters to the geometrical relationship of human body-transmitter-receiver, SNR and bandwidth of the system, clearly shows the effect of human body on TOA ranging.

The remainder of this paper is organized as follows: Section II describes the scenarios of the measurement; Section III introduces the detail of the model; Section IV presents our conclusions and comments on future work.

II. MEASUREMENT SCENARIOS

A. Measurement System

As shown in Figure 1, the measurement system employs a vector network analyzer (Agilent E8363), a pair of UWB antenna (Skycross SMT-3TO10M), low loss cables and a power amplifier (3-8GHz, 30db). The receiver (RX) antenna is used as target sensor, which is mounted to the middle of chest of human body with the height of 1.34 meters. The human involved remains standing posture during the measurement. The transmitter (TX) antenna is used as base station and it is attached to a tripod with the same height as RX antenna.

This work is supported by the National Institute of Standards and Technology (Grand # 60NANB10D001), the National Natural Science Foundation of China (Grand # 61003251 and # 61172049) and Doctoral Fund of Ministry of Education of China (Grand # 20100006110015).

In the test, S-parameter S21, the transfer function of the channel, is measured by VNA in frequency domain with 1601 sample points. The Hanning window is applied to the received signal in frequency domain to avoid the side lobes. Then, the received signal is transferred to time domain by inverse fast Fourier transform (IFFT) and the propagation time of the first detectable peak is recorded as the result of TOA ranging. The undesirable effects of the cables, the power amplifier, and antennas are removed through system calibration.

B. Settings

The measurement was performed in Room 233 of Atwater Kent Laboratory, an office building located in Worcester Polytechnic Institute, Worcester, MA, US. As shown in Figure 2, this room is medium size with dimensions of approximately 18×12 meters and filled with desks and chairs. The distance between TX and RX antenna is 5m. TOA ranging error e is defined as

$$e = \hat{d} - d \tag{1}$$

where $\hat{d}$ is the measured distance and d is the true distance .

In each test, there are three important parameters: angle between face direction and the direction of TX-RX (θ), SNR in LOS scenario without the effect of human body (SNR_{NH}) and bandwidth (W). The

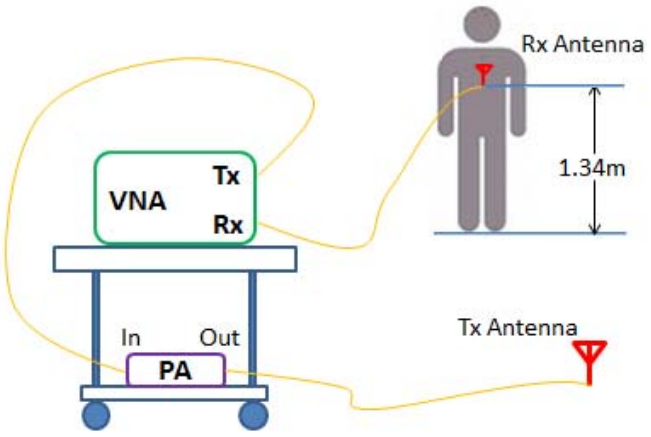

Figure 1. Measurement System

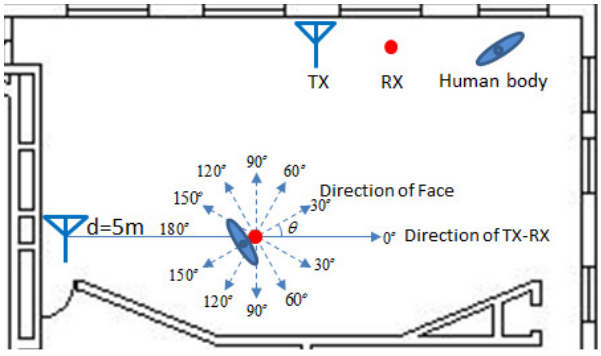

Figure 2. Test scenarios with different angles

data set of ranging error in each test can be defined as: $\hat{E}_{\theta,SNR_{NH},W}$. In each test, 600 TOA ranging errors are obtained. Definition and settings of these three parameters are introduced as follow:

(1) θ

As shown in Figure 2, the geometric relationship among human body, TX and RX is define as the angle between the face direction and the direction of TX-RX. Measurements are performed in every 30^o as shown in Figure 2. Test angles of θ are given by:

$$\theta = \{0, 30^o, 60^o, 90^o, 120^o, 150^o, 180^o\}$$

The relationship between θ and physical scenario (S) can be defined as:

$$S = \begin{cases} NLOS & \theta \in [0^o, 90^o) \\ LOS & \theta \in [90^o, 180^o] \end{cases} \tag{2}$$

(2) SNR_{NH}

In the measurements, the transmitting power (P_{TX}) of VNA is set from 0 to -40 dBm by 10dBm per step to model the effect of human body on TOA ranging error in different SNR conditions. To obtain SNR_{NH}, Rx antenna is attached to a tripod with the same height as TX antenna in the same position as depicted in Figure 2. Values of SNR_{NH} are as follows:

$$SNR_{NH} = \{71.5\,dB, 62.0\,dB, 52.4\,dB, 42.3\,dB, 32.4\,dB\}$$

(3) W

Four popular UWB bandwidths are used in our measurements to analysis the effect of bandwidth on TOA ranging error for indoor human tracking. Values of W are:

$$W = \{5\,GHz, 3\,GHz, 1\,GHz, 0.5\,GHz\}$$

III. Modeling TOA Ranging Error

A. Overview of the Effects of θ and SNR_{LOS}

The typical distributions of TOA ranging error in both LOS and NLOS scenarios of our measurements are Gaussian distributions. Figure 3 (a) and (b) show the effects of θ and SNR_{LOS} on mean and variance of TOA ranging error:

- In LOS scenarios, means and variances of TOA ranging error are similar, indicating that θ and SNR_{NH} have little effect on the distribution in LOS scenarios. It is because the direct path is the strongest path in this scenario.
- In NLOS scenarios, when θ declines, mean and variance of the TOA ranging error increase, indicates

that the effect of blockage increases as θ increases. When SNR_{NH} declines, mean and variance of the TOA ranging error increase, indicates that the effect of body-caused NLOS on TOA ranging error in low SNR condition is more serious than in high SNR condition.

B. *Modeling TOA Ranging Error for body mounted sensors*

TOA ranging error (e) of body mounted sensor can be defined as:

$$e = \varepsilon_M + \delta(P_{NLOS}(\theta)-1)\times\varepsilon_{UDP} \tag{3}$$

where ε_M is multipath error, ε_{UDP} is UDP error. $\delta(x)$ is the impulse function, given by:

$$\delta(x) = \begin{cases} 1 & x = 0 \\ 0 & x \neq 0 \end{cases} \tag{4}$$

According to (2), P_{NLOS} is defined as:

$$P_{NLOS}(\theta) = \begin{cases} 1 & \theta \in [0^o, 90^o) \\ 0 & \theta \in [90^o, 180^o] \end{cases} \tag{5}$$

(1) ε_M

According to (3), error measured in LOS is equal to multipath error:

$$e_{LOS} = \varepsilon_M \tag{6}$$

To model multipath error for body mounted sensors, the measured data of LOS scenario ($\theta \in [90^o, 180^o]$) are used to determine the distribution parameters. Our measurement result shows that for each bandwidth employed in the measurement, the ranging error forms a Gaussian distribution. Therefore the multipath error can be modeled as

$$\varepsilon_M = G(\mu_{M,W}, \sigma^2_{M,W}) \tag{7}$$

where G is a Gaussian random variable with mean $\mu_{M,W}$ and variance $\sigma^2_{M,W}$. As shown in Table I, the values of $\mu_{M,W}$ and $\sigma^2_{M,W}$ depend on the bandwidth of the system.

(2) ε_{UDP}

According to (3), ε_{UDP} can be given by:

$$\varepsilon_{UDP} = e_{NLOS} - \varepsilon_M \tag{8}$$

where e_{NLOS} is the ranging error measured in NLOS scenario. Both e_{NLOS} and ε_M correspond with Gaussian distributions. Therefore, ε_{UDP} is also modeled as a Gaussian variable, given by:

$$\varepsilon_{UDP} = G(\mu_{UDP}, \sigma^2_{UDP}) \tag{9}$$

μ_{UDP} and σ^2_{UDP} can be given by:

$$\mu_{UDP} = \mu_{NLOS} - \mu_M \tag{10}$$

$$\sigma^2_{UDP} = \sigma^2_{NLOS} - \sigma^2_M \tag{11}$$

where μ_{NLOS} is mean of e_{NLOS} and σ^2_{NLOS} is variance of e_{NLOS}. According to the value of μ_{UDP} and σ^2_{UDP} in our measurements, for a given W and SNR_{NH}, both μ_{UDP} and σ^2_{UDP} can be modeled as a linear function of $\cos^3(\theta)$ as follows:

$$\mu_{UDP} = k_1 \times \cos^3(\theta) \tag{12}$$

$$\sigma^2_{UDP} = k_2 \times \cos^3(\theta) \tag{13}$$

where k_1 and k_2 are the slope of the linear functions. Figure 4 shows the fitting results of μ_{UDP} and σ^2_{UDP} versus θ, when $W = 5GHz$. As depicted in Figure 4, k_1 and k_2 increase as SNR_{NH} declines, indicating that the effects of body-caused NLOS increase in low SNR conditions. k_1 and k_2 is modeled

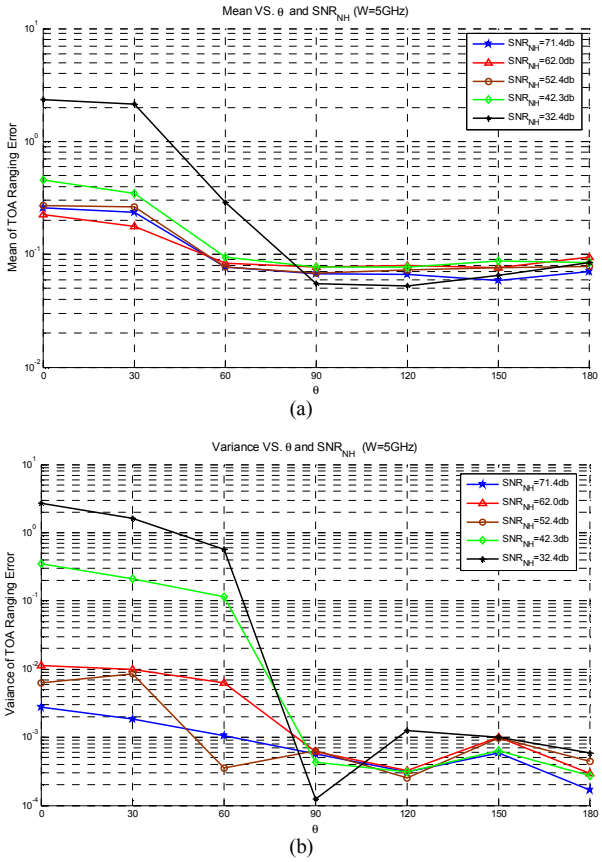

Figure 3. Effects of θ and SNR_{NH}

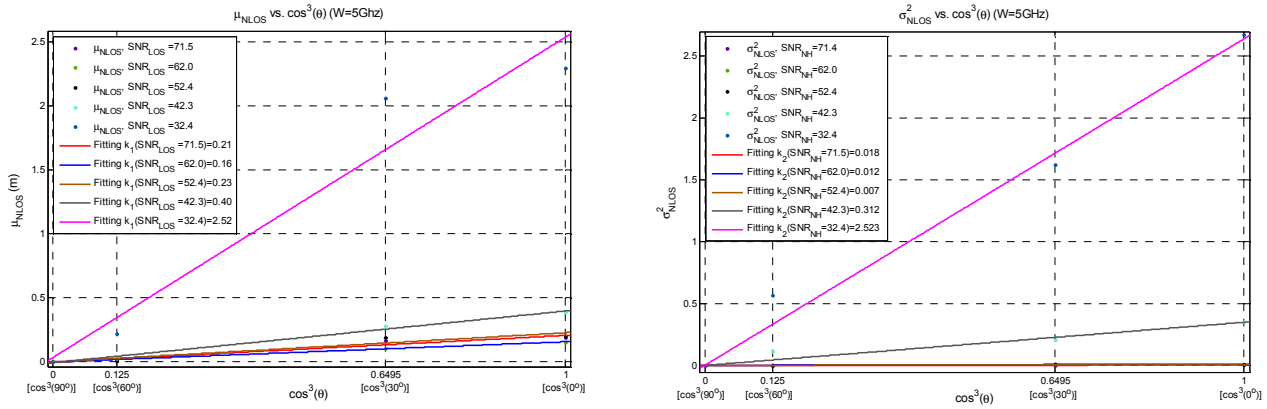

(a) (b)

Figure 4. Linear fitting μ_{UDP} and σ^2_{UDP} vs. $\cos^3(\theta)$

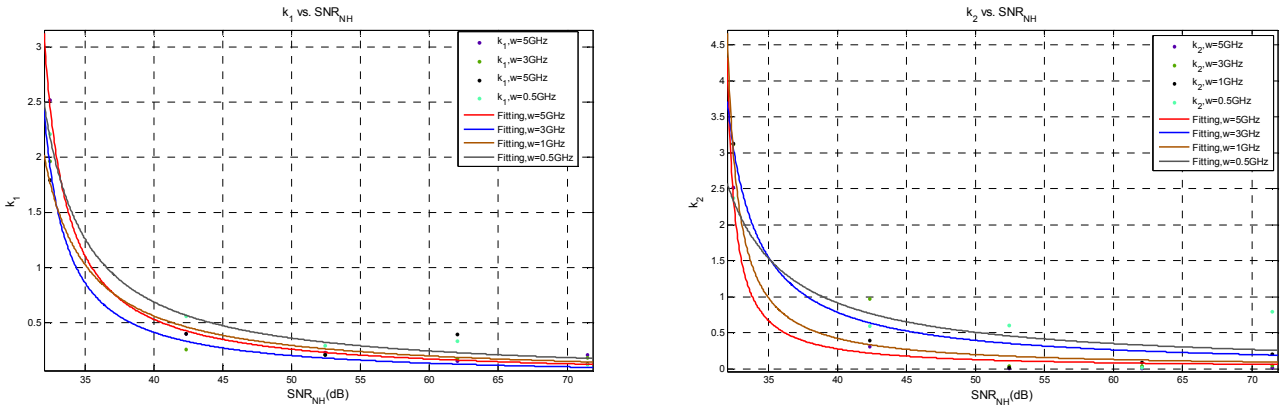

(a) (b)

Figure 5. Rational fitting k_1 and k_2 vs. SNR_{LOS}

as an inverse rational function of SNR_{NH} as follows:

$$k_1 = \frac{a_W}{SNR_{NH} - SNR_{Thre,W}} \tag{14}$$

$$k_2 = \frac{b_W}{SNR_{NH} - SNR_{Thre,W}} \tag{15}$$

where a_W, b_W and $SNR_{Thre,W}$ are the parameters depend on W. $SNR_{Thre,W}$ shows the threshold of SNR_{NH} for TOA ranging in body-caused NLOS scenario. Values of a_W, b_W and $SNR_{Thre,W}$ are shown in Table I. Figure 5 shows the fitting results of k_1 and k_2 versus SNR_{NH} when $W = 5GHz$.

According to (12), (13), (14) and (15), ε_{UDP} can be modeled as:

$$\varepsilon_{UDP} = G(\mu_{UDP,W}, \sigma^2_{UDP,W}) \tag{16}$$

where

$$\mu_{UDP,W} = \frac{a_W}{SNR_{NH} - SNR_{Thre,W}} \times \cos^3(\theta) \tag{17}$$

$$\sigma^2_{UDP,W} = \frac{b_W}{SNR_{NH} - SNR_{Thre,W}} \times \cos^3(\theta) \tag{18}$$

C. The General Model of TOA Ranging Error

According to analysis and the fitting results above, the overall model of TOA ranging error for body mounted sensors is

$$\begin{aligned} e &= \varepsilon_M + \delta(P_{NLOS}(\theta) - 1) \times \varepsilon_{UDP} \\ &= G(\mu_{M,W}, \sigma^2_{M,W}) + \delta(P_{NLOS}(\theta) - 1) \times G(\mu_{UDP,W}, \sigma^2_{UDP,W}) \end{aligned} \tag{19}$$

where $\mu_{UDP,W}$ and $\sigma^2_{UDP,W}$ are defined as (17) and (18). The values of all parameters of the model are shown in Table I. Figure 6 (a) compares the complementary CDF of the ranging error of LOS scenario with the simulated ranging error for bandwidth of 3 GHz and Figure 6 (b) compares the ranging error of NLOS scenario with the simulated ranging errors for $W = 3GHz$, $SNR_{NH} = 62.0dB$. The simulated data shows close agreement with the empirical data.

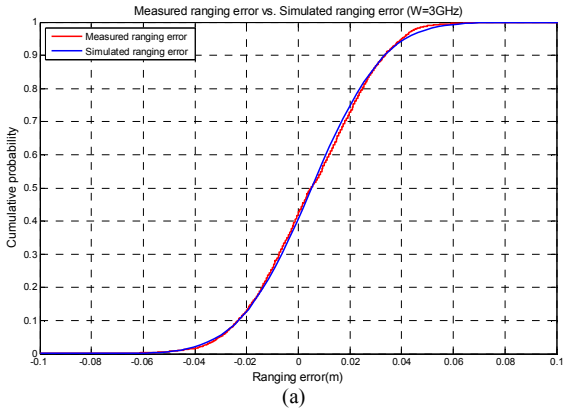

Figure 6. Measured ranging error vs. simulated ranging error

TABLE I. PARAMETERS OF THE MODEL

W (GHz)	$\mu_{M,W}$ (m)	$\sigma^2_{M,W}$	a_W	b_W	$SNR_{Thre,W}$ (db)
5	0.010	0.005	5.10	5.49	30.4
3	0.009	0.001	3.98	6.69	30.4
1	0.072	0.058	6.21	11.76	29.0
0.5	0.138	0.143	14.69	10.62	27.5

IV. CONCLUSION

In this paper, we introduce a TOA ranging error model for body mounted sensors based on the measurements in a typical office building. This model separates the ranging error into multipath error caused multipath combination and UDP error derives from body-caused NLOS. Both multipath error and UDP error are modeled as a Gaussian variable. The distribution of multipath error is relative to bandwidth of the system and the distribution of UDP error is relative to the angle between the face direction and the direction of TX-RX, SNR and bandwidth of the system, clearly shows the effects of human body on TOA ranging. The comparison between the empirical ranging error and simulated ranging error depicts in close agreement.

REFERENCES

[1] N. Moayeri, J. Mapar, S. Tompkins and K. Pahlavan, Special Issuse on Navigation Using Signals of Opportunity, IEEE Wireless Magazine, April 2011. Vol. 18, No.

[2] K. Pahlavan, X. Li, and J. Makela, "Indoor Geolocation Science and Technology", IEEE Comm Soc. Mag., Feb. 2002

[3] Jie He, Shen Li, Kaveh Pahlavan and Qin Wang, A Realtime Testbed for Performance Evaluation of Indoor TOA Location System, IEEE International Conference on Communications (ICC), Ottawa, Canada, June 10-15, 2012

[4] D. Dardari, A. Conti, U. Ferner, A. Giorgetti, and M. Z. Win, "Ranging with ultrawide bandwidth signals in multipath environments," Proc. Of IEEE, Special Issue on UWB Technology & Emerging Applications, Feb. 2009

[5] N. Alsindi, B. Alavi, K. Pahlavan, "Measurement and Modeling of Ultrawideband TOA-Based Ranging in Indoor Multipath Environments," IEEE Transactions on Vehicular Technology, Volume: 58 , Issue: 3, pp. 1046 – 1058, 2009.

[6] Heidari, M., Akgul, F. O., and Pahlavan, K., "Identification of the Absence of Direct Path in Indoor Localization Systems," International Journal of Wireless Information Networks, Volume 15, Numbers 3-4, pp. 117-127, December, 2008.

[7] Jie He, Qin Wang, Qianxiong Zhang and et, al. "A practical indoor TOA ranging error model for localization algorithm", 2011 IEEE 22nd International Symposium on Personal Indoor and Mobile Radio Communications (PIMRC), Toronto, Sep. 2011.

[8] K. Pahlavan, Y. Ye, R. Fu and U. Khan, "Challenges in Channel Measurement and Modeling for RF Localization Inside the Human Body", 2012 invited paper, Special issue on ICL-GNSS best papers, International Journal of Embedded and Real-Time Communication Systems, (in the press), Springer 2012.

[9] A. Hatami and K. Pahlavan, "Performance Comparison of RSS and TOA Indoor Geolocation Based on UWB Measurement of Channel Characteristics," 17th Annual IEEE International Symposium on Personal Indoor and Mobile Radio Communications (PIMRC'06), Helsinki, Finland, 11-14 Sept. 2006.

[10] B. Alavi and K. Pahlavan, "Modeling of the TOA based Distance Measurement Error Using UWB Indoor Radio Measurements," IEEE Communication Letters, Vol. 10, No. 4, pp: 275-277, April 2006.

[11] M. Heidari and K. Pahlavan, "A Markov Model for Dynamic Behavior of ToA-Based Ranging in Indoor Localization," EURASIP Journal on Advances in Signal Processing, vol. 2008, Article ID 241069, 14 pages, 2008.

[12] IEEE, 802.15 Tg6 ,"Draft of Channel Model for Body Area Network", November, 2010.

[13] S. Li, J. He, R. Fu and K. Pahlavan, "A Hardware Platform for Performance Evaluation of In-body Sensors" , 6th IEEE International Symposium on Medical Information and Communication Technology (ISMICT), San Diego, CA, March 26-29, 2012.

[14] R. Fu, Y. Ye, N. Yang and K. Pahlavan, "Doppler Spread Analysis of Human Motions for Body Area Network Applications", Proceedings of the 22nd annual IEEE international symposium on personal, indoor and mobile radio communications (PIMRC), September 11-14, Toronto, Canada

[15] F. Della Rosa, L. Xu, J. Nurmi, M. Pelosi, C. Laoudias, A. Terrezza, "Hand-Grip and Body-Loss Impact on RSS Measurements for Localization of Mass Market Devices", International Conference on Localization and GNSS (ICL-GNSS), 2011, pp. 58-63.